Journal of Statistical Physics, Vol. 24, No. 1, 1981

Gradient Theory of Fluid Microstructures

H. T. Davis[1] **and L. E. Scriven**[1]

Received January 8, 1980

The general gradient theory of fluid microstructures is outlined. This theory reduces the determination of fluid microstructures to a boundary value problem. The density and pressure tensor profiles and the tension of planar thin films and layered structures in one-component fluids are investigated. The boundary conditions determining these structures are given a geometric interpretation in the free energy–density diagram. Discussed are the implications of the theory for the validity of Antonov's rule, the duplex film hypothesis, and the asymptotic theory of disjoining pressure and of the origin of a characteristic length scale in spinodal decomposition.

KEY WORDS: Fluid microstructures; thin films; periodic fluid microstructures; statistical mechanics of inhomogeneous fluids; disjoining pressure.

1. INTRODUCTION

Interfacial phenomena are involved in an important way in many commercial processes and products as well as in biological mechanisms and materials. Associated with and perhaps even determinant of interfacial properties are what we call fluid microstructures. A fluid microstructure is a region in a fluid in which densities and/or compositions vary appreciably over distances of the order of magnitude of the range of molecular forces. Examples of fluid microstructures include fluid–fluid interfaces, fluid–solid interfaces, multiphase contact regions, thin films, drops and bubbles, micelles, microemulsions, liquid crystals, lipid bilayers, vesicles, foams, spinodally developing density variations, and gels.

This work was supported financially by the U.S. Department of Energy and the National Science Foundation.

[1] Departments of Chemical Engineering and Materials Science and of Chemistry, University of Minnesota, Minneapolis, Minnesota.

0022-4715/81/0100-0243$03.00/0

Fluid microstructures are ubiquitous in the products and uses of products of the emollient, detergent, coating, and processed foods industries. Foams, bubbles, drops, films (membranes), gels, and microporous solids are frequently involved in separation and reaction processes of the chemical industry as well as pollution control and water treatment industry, and the natural processes of biological systems. Capillarity, wettability, and multiphase flow in porous media are controlled to a great extent by fluid microstructures—multiphase flow phenomena in porous media are involved in natural and induced ground water movement, solution mineral leaching, petroleum recovery processes, and wood fiber treatment and manufacturing processes. Emulsion polymerization is a well-established industrial process now. Micellar or microemulsion reaction processes are under investigation for their ultimate practical utility. And liquid crystals are commonplace as watch dials and thermometers. The importance of bilayers in cellular structure and the organizational and transport processes of living matter is thoroughly established, although incompletely understood. Vesicles are under active investigation as potential vessels for drug delivery to specific sites in living organisms. The foods industry is also researching vesicle behavior for future applications.

The list of processes and systems in which fluid microstructures are consequential goes on and on and will not be produced here. What is relevant to this paper is the fact that in spite of the wide involvement of fluid microstructures in technological and natural processes and products and even though interfacial science is a classical subject, the fundamental basis for understanding the behavior of fluid microstructures still forms an exciting and developing subject. Among the objects of current theoretical interest are the local density and stress (pressure) distributions associated with the fluid microstructures; interfacial tension and other stress moments; contact angle of three-phase contact lines; film tensions, stability, and disjoining pressure; and contact angle and meniscus shape.

In this paper the density and stress profiles of several microstructures are explored with the gradient theory of inhomogeneous fluids. Gradient theory, initiated long ago by Rayleigh(1) and van der Waals[2] and more recently exploited by Cahn and Hilliard(3) and many others,[3] is strictly speaking expected to be valid only if the scale of density variations is large compared to the range of molecular forces. However, numerous theoretical(4–6) and semiempirical(7) calculations of the tension and density profiles of planar interfaces indicate that the gradient theory is a good approximation even when the scale of the density variation is only a few

---

[2] For a complete treatment of the van der Waals theory of interfaces see Ref. 2.

[3] For a bibliography of several of these see the literature citations of Ref. 3.

multiples of the range of molecular forces. Because of this fact and the relative simplicity of the gradient theory, we use it in the present paper to describe the microscopic and thermodynamic properties of planar thin films and layered (periodic) microstructures. The gradient theory of spherical microstructures will be investigated in a forthcoming publication.(5)

Although the general theory is outlined in the next section for multicomponent fluids, the computations presented in later sections are restricted to one-component fluids. Moreover, for computational simplicity many of the numerical results are given for the van der Waals fluid. However, to demonstrate that the results are qualitatively meaningful for real fluids, several computations are performed on the 6–12 Lennard-Jones fluid.

2. THE GRADIENT THEORY

The Helmholtz free energy $F(\{\mathbf{n}\})$ of an inhomogeneous fluid is a functional of the density distributions $\mathbf{n}(\mathbf{r}) \equiv (n_1(\mathbf{r}), \ldots, n_\nu(\mathbf{r}))$, where $n_\alpha(\mathbf{r})$ is the density of species α at position $\mathbf{r}$. In the absence of external fields $F(\{\mathbf{n}\})$ can be expressed in the form

$$F(\{\mathbf{n}\}) = \int f(\mathbf{r}; \{\mathbf{n}\})\, d^3r \tag{2.1}$$

where $f(\mathbf{r}; \{\mathbf{n}\})$ is the Helmholtz free energy density of the fluid at position $\mathbf{r}$. In the gradient theory, one assumes that the free energy density at $\mathbf{r}$ is a function of $\mathbf{n}$ and all gradients $\nabla\mathbf{n}$, $\nabla\nabla\mathbf{n}, \ldots,$ at $\mathbf{r}$. Then, expanding f about the homogeneous state ($\nabla\mathbf{n} = \nabla\nabla\mathbf{n} = \cdots = 0$) and retaining terms through third order in gradient, one obtains(3)

$$f(\mathbf{r}; \{\mathbf{n}\}) = f_0(\mathbf{r}) + \sum_{\alpha=1}^{\nu} \frac{1}{2} A_\alpha \nabla^2 n_\alpha + \sum_{\alpha,\beta=1}^{\nu} \frac{1}{2} B_{\alpha\beta} \nabla n_\alpha \cdot \nabla n_\beta \tag{2.2}$$

where $f_0(\mathbf{n})$ is the Helmholtz free energy density of homogeneous fluid at composition $\mathbf{n}$, and A_α and $B_{\alpha\beta}$ are quantities involving correlation functions of homogeneous fluid. Insertion of Eq. (2.2) into Eq. (2.1) and rearrangement leads to

$$F = \int \left[f_0(\mathbf{n}) + \sum_{\alpha,\beta=1}^{\nu} \frac{1}{2} c_{\alpha\beta} \nabla n_\alpha \cdot \nabla n_\beta \right] d^3r \tag{2.3}$$

where $c_{\alpha\beta} = B_{\alpha\beta} - \partial A_\alpha / \partial n_\beta$. As we shall not use A_α and $B_{\alpha\beta}$, we shall not present formulas for them here. The influence parameter $c_{\alpha\beta}$ is proportional to the square of a characteristic interparticle correlation length. In particular,(5–8)

$$c_{\alpha\beta}(\mathbf{n}) = \tfrac{1}{6} kT \int s^2 C_0^{\alpha\beta}(s; \mathbf{n})\, d^3s \tag{2.4}$$

where $C_0^{\alpha\beta}(s;\mathbf{n})$ is the direct correlation function of homogeneous fluid of composition $\mathbf{n}$. Here T is absolute temperature and k is Boltzmann's constant.

An alternative formula for $c_{\alpha\beta}$ has been derived from the gradient theory of the Yvon–Born–Green equations for an inhomogeneous fluid:$^{(9)}$

$$c_{\alpha\beta} = \frac{1}{2} u_2^{\alpha\beta} + \frac{1}{8} \sum_\gamma n_\gamma \left(\frac{\partial u_2^{\alpha\gamma}}{\partial n_\beta} + \frac{\partial u^{\beta\gamma}}{\partial n_\alpha} \right) \tag{2.5}$$

where

$$u_2^{\alpha\beta} \equiv \frac{1}{15} \int s^3 \frac{du_{\alpha\beta}^{(s)}}{ds} \, g_0^{\alpha\beta}(s;\mathbf{n}) \, d^3s \tag{2.6}$$

$u_{\alpha\beta}(s)$ is the pair potential of species α and β, and $g^{\alpha\beta}(s;\mathbf{n})$ is the pair correlation function of species α and β for homogeneous fluid at composition $\mathbf{n}$. Unlike Eq. (2.4), Eq. (2.5) is restricted to fluids whose particles interact with pairwise-additive, central forces and is based on a special approximation for the pair correlation function of inhomogeneous fluid, namely,

$$g^{\alpha\beta}(\mathbf{r},\mathbf{r}') = g_0^{\alpha\beta}\left(|\mathbf{r} - \mathbf{r}'|; \mathbf{n}\left(\frac{\mathbf{r} + \mathbf{r}'}{2} \right)\right) \tag{2.7}$$

Although Eq. (2.5) is based on this inexact correlation function, we have found$^{(10)}$ that predictions of density profiles and surface tensions of the 6–12 Lennard-Jones model using Eq. (2.5) agree quite well (say 10% discrepancies) with those obtained using Eq. (2.4). The reason appears to be that $c_{\alpha\beta}$ of Eq. (2.4) and $u_2^{\alpha\beta}$ are weak functions of density. In the dilute gas limit Eqs. (2.4) and (2.5) are identical.

An advantage of introducing the approximate pair correlation function (2.7) and focusing on two-body central forces is that the gradient theoretical pressure tensor P can be obtained directly from the Bearman–Kirkwood theory.$^{(11)}$ Through third order in gradients, the pressure tensor corresponding to Eq. (2.7) is$^{(9)}$

$$\begin{aligned} \mathsf{P} = P_0(\mathbf{n})\mathsf{I} - \sum_{\alpha,\beta=1}^{\nu} \frac{1}{12} \square : \Big\{ & \frac{1}{4} n_\alpha n_\beta \nabla\nabla u_2^{\alpha\beta} \\ & + \frac{1}{2} (n_\beta \nabla n_\alpha + n_\alpha \nabla n_\beta) \nabla u_2^{\alpha\beta} \\ & + \left[n_\beta \nabla\nabla n_\alpha - (\nabla n_\alpha)(\nabla n_\beta) + n_\alpha \nabla\nabla n_\beta \right] \Big\} \end{aligned} \tag{2.8}$$

where $P_0(\mathbf{n})$ is the pressure of homogeneous fluid at composition $\mathbf{n}$,

$$P_0(\mathbf{n}) = \sum_{\alpha=1}^{\nu} n_\alpha kT = \sum_{\alpha,\beta=1}^{\nu} \frac{1}{6} \int s \frac{du_{\alpha\beta}}{ds} \, g_0^{\alpha\beta}(s;\mathbf{n}) \, d^3s \tag{2.9}$$

and $\square$ is a fourth-rank tensor of the form

$$\square = \mathsf{II} + \sum_{i,j=1}^{3} (\hat{\mathbf{e}}_i\hat{\mathbf{e}}_j\hat{\mathbf{e}}_j\hat{\mathbf{e}}_i + \hat{\mathbf{e}}_i\hat{\mathbf{e}}_j\hat{\mathbf{e}}_i\hat{\mathbf{e}}_j) \tag{2.10}$$

$\hat{\mathbf{e}}_i$ is the ith unit vector of a Cartesian basis set, and $\mathbf{I}$ is the unit tensor.

The rigorous gradient theory of the pair correlation function has been worked out,$^{(12)}$ so that in principle the rigorous gradient formula for P can be used instead of Eq. (2.8). However, the result is a complicated expression involving second-, third-, and fourth-order direct correlation functions, which are not available for computation.

For a closed isothermal system, equilibrium microstructures are those that minimize the Helmholtz free energy. The density distributions for which Eq. (2.3) is an extremum can be shown by standard calculus of variations to obey the set of equations$^{(3)}$

$$\sum_{\beta=1}^{\nu} \nabla\cdot(c_{\alpha\beta}\nabla n_\beta) - \frac{1}{2}\sum_{\gamma,\beta=1}^{\nu} \frac{\partial c_{\gamma\beta}}{\partial n_\alpha}\nabla n_\gamma\cdot\nabla n_\beta = \frac{\partial\omega}{\partial n_\alpha} \tag{2.11}$$

$\alpha = 1, \ldots, \nu$, where ω is a thermodynamic potential defined by

$$\omega(\mathbf{n}) = f_0(\mathbf{n}) - \sum_\alpha n_\alpha \mu_\alpha \tag{2.12}$$

μ_α is the chemical potential of species α.

With Eq. (2.11) the determination of a given fluid microsctructure becomes the task of solving a nonlinear boundary value problem. The existence of a microstructure is largely governed by the thermodynamic potential ω (and therefore the Helmholtz free energy density f_0 of homogeneous fluid) and the characteristic length scales are controlled primarily by the influence parameters. Whether a given microstructure determined by the extremal equations (2.11) is locally stable depends on whether the density distriubutions minimize the free energy. Stability depends significantly on f_0 and $c_{\alpha\beta}$.

In the case of a planar system, $n_\alpha = n_\alpha(x)$, Eq. (2.11) can be multiplied by dn_α/dx, summed, and integrated to yield

$$\sum_{\alpha,\beta} \frac{1}{2} c_{\alpha\beta} \frac{dn_\alpha}{dx}\frac{dn_\beta}{dx} = \omega(\mathbf{n}) + K \tag{2.13}$$

where K is a constant of integration. Let us define the tension γ of the planar system by

$$\gamma = \left(\frac{\partial F}{\partial A}\right)_{T,V,\mathrm{N}} \tag{2.14}$$

A is the area of the system in the plane normal to the x direction, V is the volume, and $\mathrm{N} \equiv (N_1, \ldots, N_\nu)$, with $N_\alpha = \int n_\alpha\, d^3r$. Combining Eqs. (2.3) and (2.13), we obtain

$$\gamma = \int \sum_{\alpha,\beta} c_{\alpha\beta} \frac{dn_\alpha}{dx} \frac{dn_\beta}{dx} dx \tag{2.15}$$

From Eq. (2.8) we obtain for a planar system an interesting relationship between the normal pressure component $P_N \equiv P_{xx}$ and the transverse pressure component $P_T \equiv P_{zz} = P_{yy}$, namely,$^{(9)}$

$$P_T = \tfrac{2}{3} P_0(\mathbf{n}) + \tfrac{1}{3} P_N \tag{2.16}$$

In the absence of an external field P_N is constant for a planar system. Thus, according to Eq. (2.16) the variation of the transverse component of pressure with density variation of the microstructure is governed by the equation of state of homogeneous fluid.

In the great majority of microstructured fluids there are ions present, and related double layer phenomena. Electrostatic fields and conservative external fields can be included in the gradient theory by expressing the Helmholtz free energy in the form$^{(13)}$

$$F(\{\mathbf{n}\}) = \int \left[f_0(\mathbf{n}) + \sum_{\alpha,\beta} \frac{1}{2} c_{\alpha\beta} \nabla n_\alpha \cdot \nabla n_\beta + \sum_\alpha n_\alpha u_e^\alpha(\mathbf{r}) + \frac{1}{8\pi} \epsilon E^2 \right] d^3r \tag{2.17}$$

where u_e^α is the potential of any nonelectrostatic external forces present, $\mathbf{E}$ is the electric field, and ϵ is the dielectric constant. We assume ϵ is a known function of $\mathbf{n}$. The electric field at $\mathbf{r}$ is the negative of the gradient of the voltage $\psi(\mathbf{r})$ (i.e., $\mathbf{E} = -\nabla\psi$), which obeys the Poisson equation

$$\nabla \cdot (\epsilon \nabla \psi) = -4\pi \sum_\alpha z_\alpha e n_\alpha \tag{2.18}$$

e is the unit electronic charge and z_α is the valence of species α. The extremal equations obeyed by equilibrium microstructures are

$$\begin{aligned} \sum_{\beta=1}^{\nu} \nabla \cdot (c_{\alpha\beta} \nabla n_\beta) - \frac{1}{2} \sum_{\gamma,\beta=1}^{\nu} \frac{\partial c_{\gamma\beta}}{\partial n_\alpha} \nabla n_\gamma \cdot \nabla n_\beta \\ = \frac{\partial \omega}{\partial n_\alpha} + u_e^\alpha - \frac{1}{8\pi} \frac{\partial \epsilon}{\partial n_\alpha} E^2 + z_\alpha e \psi \end{aligned} \tag{2.19}$$

The quantity $-(1/8\pi)(\partial\epsilon/\partial n_\alpha)E^2$ represents the contribution of electrostriction to the chemical potential. It is usually ignored in double layer theories because it is small except at very high electric fields. Sufficiently near a critical point this contribution could be appreciable compared to $\partial\omega/\partial n_\alpha$ and therefore play an important role in near-critical microstructures.

3. THIN FILMS

We consider here planar thin films of one-component fluids. For purposes of discussion thin films can be conveniently divided into two classes: (1) thin phases, i.e., films that are thick enough to behave as a bulk phase with two interfaces characterized by bulk phase tensions, and (2) thin films, whose tension depends on film thickness. We shall investigate class 2 films to determine (a) the thermodynamic conditions under which such films are solutions of the extremal equation, (b) what controls film density and stress profiles and tension, (c) how thick a film must be to behave as a thin phase, and (d) whether thin films are local minima of the free energy.

The boundary conditions defining a one-component thin film are that the density be maximum (liquid-like film) or minimum (gas-like film) at the center and that n tend to a bulk value n_B as $x \to \pm\infty$, i .e.,

$$\left.\frac{dn}{dx}\right|_{x=0} = 0, \qquad n \to n_B \quad \text{as } x \to \pm\infty \tag{3.1}$$

Referring back to the one-component, planar versions of Eqs. (2.11) and (2.13), we find that these conditions require

$$\omega(n_B) + K = \omega(n_0) + K = 0$$

or

$$-K = \omega(n_0) = \omega(n_B) \tag{3.2}$$

and

$$\left.\frac{\partial \omega}{\partial n}\right|_{n=n_B} = 0$$

or

$$\mu = \mu_0(n_B) \tag{3.3}$$

n_0 $[\equiv n(x=0)]$ is the density at the film center. If at a given temperature T, the bulk density n_B is set, then Eqs. (3.2) and (3.3) determine the chemical potential μ and the density n_0. More generally, setting values for any two of the quantities T, n_B, n_0, and μ fixes the state of a thin film.

The density profile of the film can be obtained by solving Eq. (2.16) for dx,

$$dx = \left(\frac{c}{2}\right)^{1/2} \frac{dn}{\left[\omega(n) - \omega(n_B)\right]^{1/2}} \tag{3.4}$$

and integrating

$$x = \int_{n_0}^{n(x)} \left(\frac{c}{2}\right)^{1/2} \frac{dn}{\left[\omega(n) - \omega(n_B)\right]^{1/2}} \tag{3.5}$$

The film tension can be computed from any of the following formulas:

$$\begin{aligned}\gamma &= \int_{-\infty}^{\infty} c\left(\frac{dn}{dx}\right)^2 dx \\ &= 2\int_{-\infty}^{\infty}\left[\omega(n)-\omega(n_B)\right]dx \\ &= 2\int_{\min[n_0,n_B]}^{\max[n_0,n_B]}\left\{2c\left[\omega(n)-\omega(n_B)\right]\right\}^{1/2}dn \qquad (3.6)\end{aligned}$$

For a planar interface to be stable the quantity c must be a positive function of density. Calculations with the 6–12 Lennard-Jones potential yield a positive c that is a weak function of density (and temperature). Since c is positive, thin films can occur only if $\omega(n)-\omega(n_B)>0$ for $\min[n_0,n_B]<n<\max[n_0,n_B]$. Otherwise, the rhs of Eq. (3.4) would be imaginary, a physically impossible result. Whether this positivity condition on $\Delta\omega(n)\equiv\omega(n)-\omega(n_B)$ can be met depends on the Helmholtz free energy density of homogeneous fluid. Qualitative plots of $f_0(n)$ versus density are presented in Fig. 1 for the cases $T>T_c$ and $T<T_c$. From the plots $\Delta\omega(n)$ in the figure, we see that the following geometric construction determines the existence of a thin film corresponding to bulk density n_B:

(a) The chemical potential μ is the tangent of $f_0(n)$ at n_B.

(b) Draw a line tangent to and touching $f_0(n)$ and n_B. The ordinate of this line is $n\mu+\omega(n_B)$.

(c) $\Delta\omega(n)$ is the vertical distance from the line to the curve $f_0(n)$.

(d) If the line intersects $f_0(n)$ at some n_0 and if $\Delta\omega(n)$ is positive between n_B and n_0, then a thin film exists with centerline density n_0 and bulk density n_B.

For temperatures above T_c there exists no n_B such that the tangent $n\mu+\omega(n_B)$ intersects the curve $f_0(n)$. Thus, no thin films exist at supercritical temperatures. On the other hand, for $T<T_c$, there are infinitely many thin films, corresponding to two ranges of n_B. As illustrated in Fig. 2, there is a range of bulk densities for which liquid-like thin films occur (this is $n_g<n_B<n_{gs}$), and there is a range of bulk densities for which gas-like thin films occur (this is $n_{ls}<n_B<n_l$). Here n_g and n_l are densities of the bulk vapor and liquid phases in thermodynamic equilibrium. For values of n_B less than n_g and greater than n_l, no thin film occurs. The density n_{gs} locates the gas side of the spinodal curve and n_{ls} locates the liquid side of the spinodal curve (generated by the equation $\partial^2 f_0/\partial n^2=0$). That there are no thin film states for n_B in the range $n_{gs}<n_B<n_{ls}$ is simply a reflection of the fact that homogeneous fluid is unstable in this density range. It is important to note, however, that some of the densities in the inhomogeneous portion of the film can lie between n_{gs} and n_{ls} (similarly to liquid–

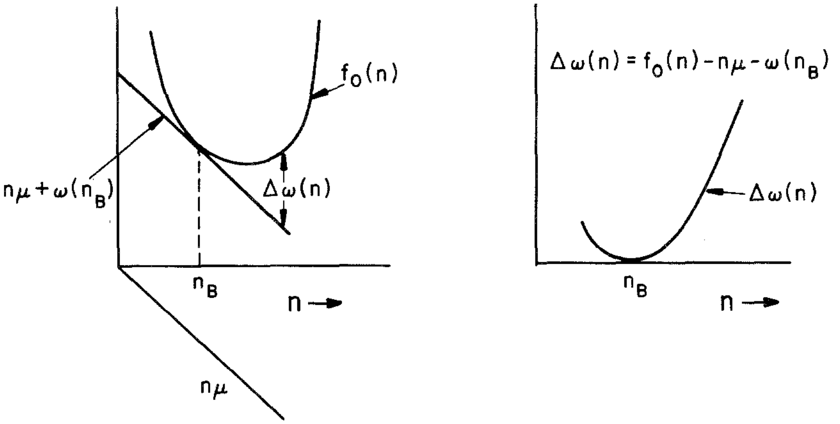

(a) $T > T_c$

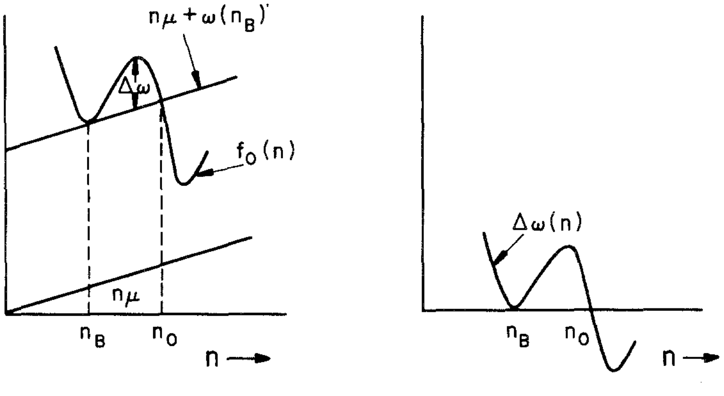

(b) $T < T_c$

Fig. 1. Free energy construction of the density in the center and in the bulk region of a symmetric thin film.

vapor interfaces). Such density states are stabilized by the density gradients in the film or interfacial regions.

To summarize: If $T > T_c$, thin films do not occur. If $T < T_c$, then families of thin films exist, the one being liquid-like and having bulk densities in the range $n_g < n_B < n_{gs}$ and the other being gas-like and having bulk densities in the range $n_{ls} < n_B < n_l$. The saturated liquid and vapor densities n_g and n_l and the liquid-side and vapor-side spinodal densities n_{ls} and n_{lg} are determined by the temperature T. Once T is set, a particular thin film is fixed by setting n_B, n_0, or μ.

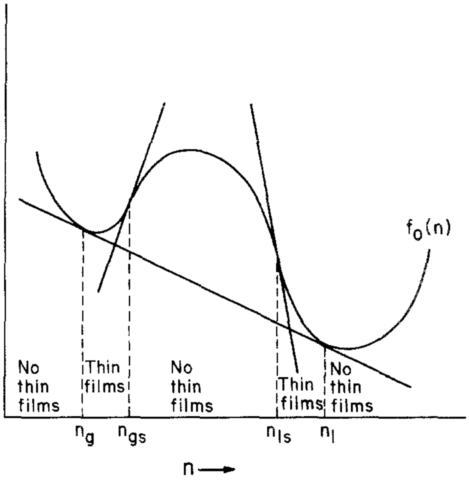

Fig. 2. Ranges of bulk densities of thin films at a subcritical temperature.

One can anticipate from Eqs. (3.5) and (3.6) and the geometrical constructions in Figs. 1 and 2 the qualitative behavior of thin films with T and n_B. As T approaches T_c, $f_0(n)$ becomes flatter between n_g and n_l, so that $\Delta\omega(n)$ becomes smaller. Thus, for a given n_B the film width tends to increase and the tension to decrease as T approaches T_c. And for a fixed T, as n_B approaches n_{gs} for a liquid-like film or n_{ls} for a gas-like film, $\Delta\omega(n)$ decreases and the film tension decreases correspondingly. At a given T, as n_B tends to n_g (or n_l), n_0 tends to n_l (or n_g), the film becomes infinitely wide, and the film tension approaches twice the surface tension of the saturated liquid–vapor interface. Thus, the liquid–vapor interface can be viewed as one of the interfaces of an infinitely thick film.

To appreciate more quantitatively the dependence of thin films on n_B (or on μ) and to answer the question of how thick a thin film must be before it begins to behave as a thin phase, we have carried out a number of computations for a van der Waals fluid and the 6–12 Lennard-Jones fluid. We discuss first a van der Waals fluid, whose Helmholtz free energy formula is

$$f_0(n) = n\mu^\dagger(T) - nkT\left[\ln(1/n - b) + 1\right] - na^2 \tag{3.7}$$

$u^\dagger(T)$ arises from the internal energy of the molecules—it cancels out of all of our (isothermal) computations; a is an energy-related constant and b is a constant accounting for the excluded volume of fluid particles; $\mu_0(n)$ is equal to the derivative of $f_0(n)$ with respect to n, and

$$P_0(n) = nkT/(1 - nb) - na^2 \tag{3.8}$$

Consistent with van der Waals' model we assume c is constant. Calculations are carried out and the results reported in the dimensionless variables

$$n^* = nb, \qquad T^* = bkT/a, \qquad P^* = b^2P/a, \qquad \omega^* = b^2\omega/a$$
$$\gamma^* = b^2\gamma/(ac)^{1/2}, \qquad f_0^* = b^2 f_0/a, \qquad \mu^* = b\mu/a, \qquad x^* = (a/c)^{1/2}x \tag{3.9}$$

The quantity $(c/a)^{1/2}$ has dimensions of length and is proportional to the range of intermolecular forces. In the reduced variables used here $T^* = 0.296$ at the critical point.

Four examples of thin-film density profiles are presented in Fig. 3, two being films of greater density than bulk phase (liquid-like films) and two of density less than bulk phase (gas-like films). The reduced temperature is $T^* = 0.223$ in all cases. At this temperature saturated liquid and vapor densities are 0.679 and 0.0600. The liquid-like film with $n_B = 0.06004$, though still very thin on a macroscopic scale, has a liquid interior that is essentially saturated bulk liquid. To answer the question of when a thin film is thick enough to behave as a bulk phase with two interfaces, let us introduce for convenience the criteria that a thin film has become a thin layer of a phase when: (i) n_0 is within 1% of the saturated bulk liquid (or vapor) value and (ii) the film tension is within 1% of twice the surface tension of the planar interface. With these criteria, we conclude from the entries in Table I that remarkably thin films behave as bulk phase. For the example given in Table I, a thin film behaves as bulk phase when its

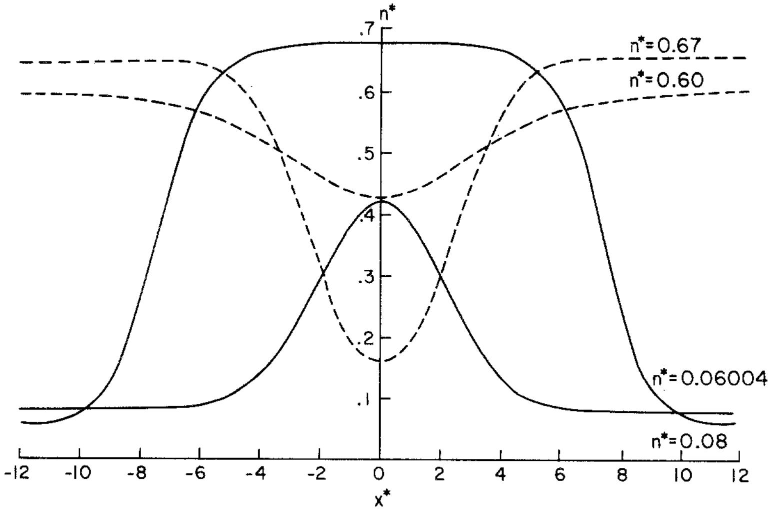

Fig. 3. Density profiles of thin films of a van der Waals fluid at $T^* = 0.223$.

Table I. The Reduced Center and Bulk Densities, Half-Width Film Tension, and Chemical Potentials of Thin Films of a van der Waals Fluid at $T^* = 0.223$[a]

n_0^*	n_B^*	$\Delta x_{1/2}^*$	γ^*	μ^*
0.32243	0.100	2.764	0.0181	− 0.6652
0.42757	0.080	2.531	0.0506	− 0.6853
0.50527	0.070	2.561	0.0819	− 0.7000
0.55976	0.065	2.699	0.1049	− 0.7091
0.62937	0.061	3.220	0.1307	− 0.7172
0.64524	0.0605	3.501	0.1350	− 0.7183
0.65974	0.0602	3.930	0.1379	− 0.7189
0.667	0.0601	4.351	0.1389	− 0.7191
0.67878	0.0600432	7.421	0.1397	− 0.7193
0.679	0.0600	+ ∞	0.142	− 0.7194
0.158747	0.67	2.681	0.1052	− 0.72932

[a] The datum of the chemical potential is $\mu^+(T)$.

half-width $\Delta x_{1/2}$, defined by the expression

$$\Delta x_{1/2}^* = \frac{1}{2} \int_{\min[n_0,(n_0^*+n_B^*)/2]}^{\max[n_0^*,(n_0^*+n_B^*)/2]} \frac{dn^*}{\left[\omega^*(n^*) - \omega^*(n_B^*)\right]^{1/2}} \tag{3.10}$$

is about four times the quantity $(c/a)^{1/2}$, or roughly four times the range of molecular interactions. Actually, the important length scale is the thickness of the planar liquid–vapor interface. If the half-width of the film is a couple of multiples of this width, the film behaves essentially as a thin layer of a bulk phase.

We also examined thin films for the 6–12 Lennard-Jones model, i.e., for a fluid whose particles interact with the pair potential

$$u(s) = 4\epsilon\left[(\sigma/s)^{12} - (\sigma/s)^6\right] \tag{3.11}$$

The Weeks–Chandler–Andersen theory(14) was used to compute $f_0(n)$ and the pair correlation function of a homogeneous fluid. Equation (2.5) was used for computing c. The results are reported in the following reduced variables:

$$n^r = n\sigma^3, \qquad T^r = kT/\epsilon, \qquad x^r = x/\sigma, \qquad \gamma^r = \sigma^2\gamma/\epsilon \tag{3.12}$$

At the critical point $T^r = 1.4$ for the theoretical free energy function we used.

In Fig. 4 the density profiles of several liquid-like thin films are plotted for films at reduced temperature $T^r = 0.703$. As was the case for the van der Waals fluid, thin films of the Lennard-Jones fluid are essentially thin phases at quite small half-widths. This is verified in Table II for tempera-

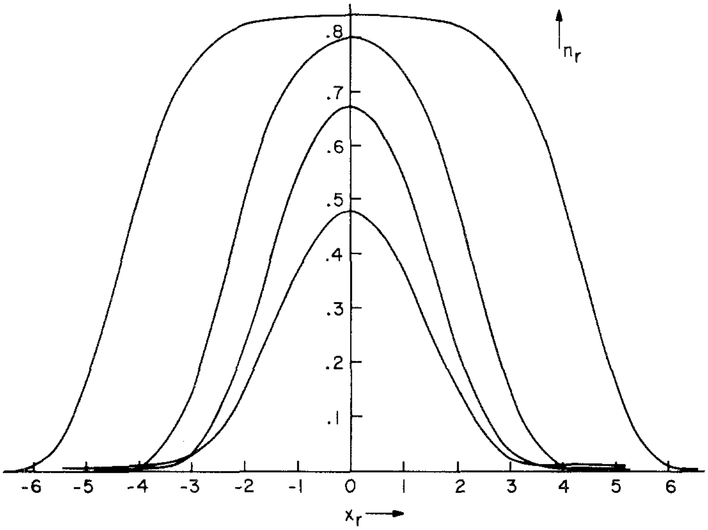

Fig. 4. Density profiles of thin films of a 6–12 Lennard-Jones fluid at $T^r = 0.703$.

tures ranging from near the triple point up to within a few percent of the critical point. Comparing the results of Table II and theoretical profiles of liquid–vapor interfaces of the 6–12 Lennard-Jones fluid, we conclude that for this fluid, too, a thin film behaves as a thin phase if its half-width is a couple of multiples of the width of the liquid–vapor interfacial zone.

That such thin films can behave essentially as phases has a bearing on Antonov's rule.(15) For many three-phase systems it has been observed that the interfacial tension between a pair of them, say phases 1 and 3, is equal to the sum of the interfacial tensions between phases 1 and 2 and phases 2 and 3, i.e.,

$$\gamma_{13} = \gamma_{12} + \gamma_{23} \tag{3.13}$$

An explanation of this relationship is that a thin film of phase 2 forms spontaneously between phases 1 and 3 when they are contacted, so that the observed tension is that of the two interfaces of the thin film. Since the film is not generally observed in the tension studies, this explanation of Antonov's rule can be valid only if the thin film of phase 2, though thick enough to behave as a bulk phase, is small compared to the resolution of visible light. For the model calculations reported here, bulk-like films would certainly be invisible except near the critical point.

It has been discovered that ultralow tension between oil and water at low surfactant concentration occurs for certain surfactants only if a finely

Table II. Reduced Maximum Density n_0^r, Bulk Density n_B^r, Half-Width D$x_{1/2}^r$, Film Tension γ^r, and Chemical Potential μ^r for Liquid-Like Thin Films of a 6–12 Lennard-Jones Fluid of Classical Monatomic Particles (Having the Molecular Weight of Argon)

n_0^r	n_B^r	$\Delta x_{1/2}^r$	γ^r	μ^r
$T^r = 0.703$				
0.842	0.00202	∞	3.026	−4.366
0.799	0.00212	4.56	2.942	−4.345
0.772	0.00222	4.06	2.784	−4.313
0.671	0.00302	3.4	2.279	−4.102
0.606	0.00403	3.2	1.865	−3.908
0.474	0.00807	3.17	1.071	−3.453
0.402	0.0121	3.28	0.711	−3.201
0.352	0.0161	3.33	0.498	−3.031
0.313	0.0202	3.48	0.359	−2.908
0.191	0.0403	4.27	0.0722	−2.590
0.0954	0.0706	9.10	0.00084	−2.459
$T^r = 1.029$				
0.702	0.0314	∞	1.322	−3.781
0.692	0.03144	8.13	1.318	−3.780
0.699	0.0317	6.37	1.285	−3.773
0.592	0.0346	4.90	1.065	−3.706
0.449	0.471	4.43	0.546	−3.477
0.347	0.0628	4.64	0.247	−3.297
0.289	0.0754	5.02	0.125	−3.203
0.222	0.0942	6.04	0.0357	−3.102
$T^r = 1.374$				
0.485	0.1634	∞	0.124	−3.4783
0.473	0.1636	16.04	0.122	−3.478
0.447	0.165	12.21	0.109	−3.475
0.397	0.172	10.41	0.073	−3.462
0.357	0.180	10.32	0.043	−3.449
0.278	0.204	13.56	0.0052	−3.425
0.257	0.212	16.77	0.0016	−3.422

dispersed third phase is present. The simplest hypothesis to explain this finding is that a thin, invisible film of the third phase gives rise to the observed ultralow tension between the oil and water phases.

Our calculations also support the duplex film hypothesis of Harkins.(16) According to this hypothesis, for films of molecular scale thickness the surface excess Helmholtz free energy of a solid–film–gas interface is equal to the sum of the solid–bulk liquid surface excess free energy and the bulk liquid–gas surface tension. Gradient theory provides a precise way of determining when a thin film becomes a duplex film.

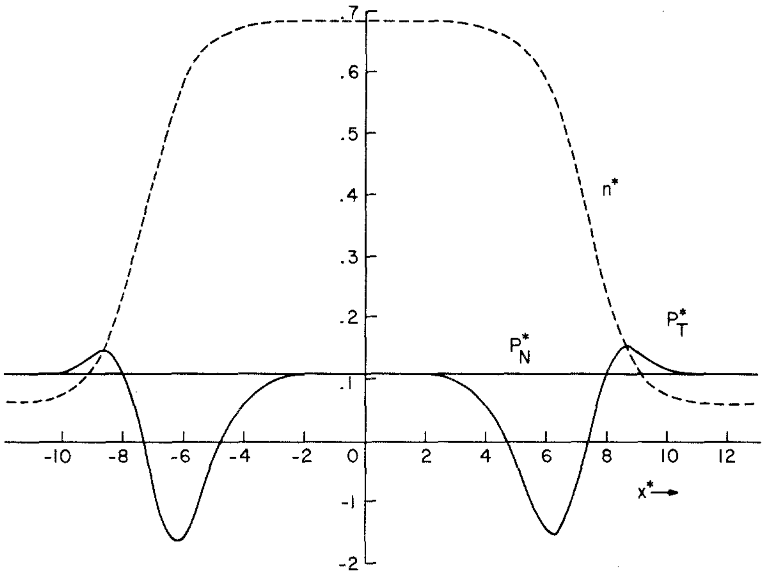

Fig. 5. Density and transverse and normal pressure profiles of a thin film of a van der Waals fluid at $T^* = 0.223$.

Another interesting property of a thin film is the pressure tensor. There are two components for a planar film: (1) the normal component P_N, which is constant across the film and is equal to the bulk pressure [i.e., $P_N = P_0(n_B)$] and (2) the transverse component P_T. The tension of the film is the integral across the film of their difference, i.e., $\gamma = \int_{-\infty}^{\infty}(P_N - P_Y)\,dy$. According to gradient theory, P_T is given by

$$P_T = \tfrac{2}{3}P_0(n) + \tfrac{1}{3}P_N \tag{3.14}$$

In Fig. 5 the density profile and corresponding pressure profiles are plotted for a thin film of a van der Waals fluid. The film interface is under tension ($P_T < P_N$) on the liquid-like side of the film interface and is under compression on the gas-like side of the interface. The transverse pressure is actually negative across part of the interface. In gradient theory the negative pressure comes from negative values of $P_0(n)$ that occur in the van der Waals loop between vapor and liquid densities. As illustrated in Fig. 6 for a van der Waals fluid, negative pressures appear at quite high temperatures (in fact for $T^* \leqslant 1/4$ for the VDW equation: $T^*_{\text{critical}} = 0.296$). In the *PVT* diagrams of most textbooks the region of negative pressures is usually not discussed. For bulk fluid it does not seem to be very important. However, in inhomogeneous fluid the negative region plays an important role in the properties of the microstructure. At very low temperatures the

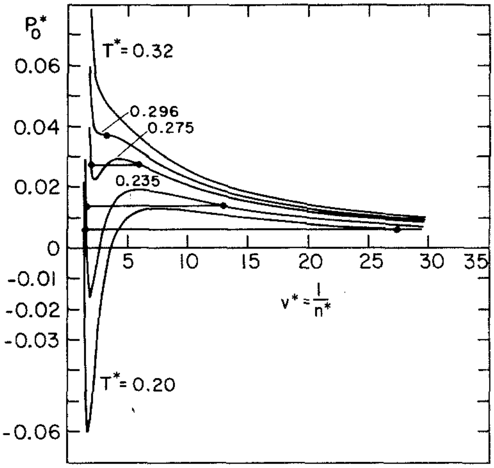

Fig. 6. *PVT* phase diagram of a van der Waals fluid. The liquid–vapor densities are indicated by the points connected with constant-pressure tie-lines.

negative region of P_T accounts for most of the tension of an interface. Adjacent tensile and compressive zones of P_T give rise to bending moments. In the case of the symmetric thin films studied here, the bending moments cancel. However, for a thin film between unlike phases the bending moments may determine the natural curving tendencies of the thin film. And in curved films, e.g., vesicles and liposomes, the bending moments may affect stability. The role of the state of stress in fluid microstructure deserves a great deal of attention in the future.

In the colloid literature the state of a thin film is sometimes represented by its disjoining pressure Π, defined by(17–19)

$$\Pi = P_N - P_R \tag{3.15}$$

where P_N is the normal pressure of the thin film and P_R is the pressure of bulk phase of the film material at the same temperature and chemical potential as the film. We shall refer to this as the reference phase. Rusanov and Kuni(20) have developed an asymptotic (valid for sufficiently thick films) theory of a planar film of width H bounded on its two faces by phases of uniform densities n_1 and n_2. Under the assumption that the film molecules interact with each other and with the bounding phases via the 6–12 Lennard-Jones pair potential, Rusanov and Kuni (RK) showed that the disjoining pressure and the difference between the center film density n_0 and the reference density n_R vary as H^{-3} for sufficiently thick films. In particular, they find for a one-component film

$$\Pi = BH^{-3} + O(H^{-4}) \tag{3.16}$$

and

$$n_0 - n_R = -\tfrac{1}{6}\pi n_R^2 K_T^R (n_1 A_{f1} + n_2 A_{f2} - 2n_R A_{ff}) H^{-3} + O(H^{-4}) \quad (3.17)$$

where

$$B = \tfrac{1}{6}\pi\left(n_R n_1 A_{f1} + n_R n_2 A_{f2} - n_R^2 A_{ff} - n_1 n_2 A_{12}\right) \quad (3.18)$$

The A_{ij} are Hamaker constants for the pair interactions among film and boundary phase molecules [$A = 4\epsilon\sigma^6$ in the notation of Eq. (3.11)] and K_T^R is the isothermal compressibility of the reference phase.

For the unsupported thin films of the 6–12 Lennard-Jones fluid considered in the present work, $A_{f1} = A_{f2} = A_{ff} = A_{12} = 4\epsilon\sigma^6$ and the densities n_1 and n_2 of the uniform bounding phases are equal to n_B, so that

$$\Pi = -\tfrac{2}{3}\pi\epsilon\sigma^6 (n_R - n_B)^2 H^{-3} \quad (3.19)$$

and

$$n_0 - n_R = -32\pi\epsilon\sigma^6 n_R^2 K_T^R (n_R - n_B) H^{-3} \quad (3.20)$$

Since the unsupported thin films of the present work approach a uniform density n_B asymptotically, there is some difficulty in identifying the film width H. For convenience we shall identify H with twice the half-width defined by Eq. (3.10). For films wide compared to the width of the vapor–liquid interfacial zone, this assignment of H is reasonable—it is for such wide films that the RK asymptotic theory is applicable. For films supported between two solid phases, one can vary H while holding fixed the temperature and chemical potential of the film phase. Equations (3.16) and (3.17) can therefore be tested at constant n_R and K_T^R. For our unsupported film, we must vary the chemical potential to vary the width of the film. Thus, n_R, K_T^R, and n_B vary with film width. However, for films wide compared to the width of the liquid–vapor interfacial zone, these quantities vary slowly, so that one may still expect the RK results to hold.

We have computed Π and $n_0 - N_R$ for liquid-like films of the 6–12 Lennard-Jones fluid at $T^r = 0.875$ and 1.117. The Weeks–Chandler–Andersen theory was used for the Helmholtz free energy and pair correlation function of a homogeneous fluid. The properties of a thin film are fixed by setting T and $\mu = \mu_0(n_B)$. The density of the reference phase is given by $\mu = \mu_0(n_R)$. There are actually three densities satisfying $\mu = \mu_0(n)$. These are n_B, n_R, and n_u, n_u being intermediate between n_B and n_R and corresponding to unstable homogeneous fluid. The reference pressure is computed from $P_R = P_0(n_R)$; and $K_T^R = [(1/n)\,\partial n/\partial P_0(n)]_{n=n_R}$.

Results of gradient theory for $n_R^r - n_0^r$ are presented in Figs. 7 and 8, where $(n_R^r - n_0^r)^{1/3}$ is plotted versus $1/\Delta x_{1/2}^r$. As expected, for sufficiently wide films ($x_{1/2} \geqslant 5\sigma$ for $T^r = 0.875$ and $\Delta x_{1/2} \geqslant 10\sigma$ for $T^r = 1.117$),

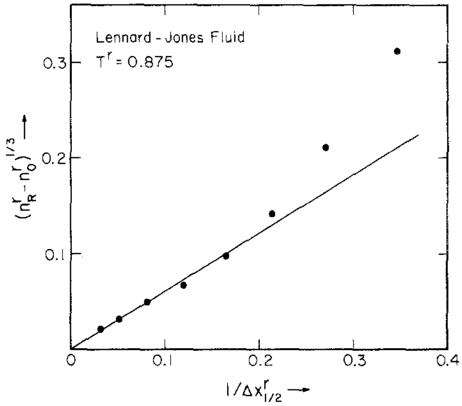

Fig. 7. Cube root of the difference between the gradient-theoretical film center density and reference bulk fluid density versus the film half-width for a 6–12 Lennard-Jones fluid. The straight line coincides with the RK theory.

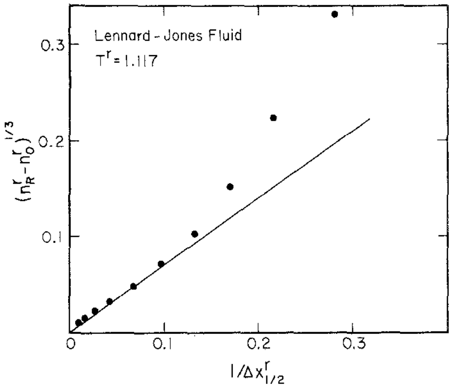

Fig. 8. Cube root of the difference between the gradient-theoretical film center density and reference bulk fluid density versus the film half-width for a 6–12 Lennard-Jones fluid. The straight line coincides with the RK theory.

$(n_R^r - n_0^r)^{1/3}$ is a linear function of $1/\Delta x_{1/2}^r$. At $T^r = 0.875$, the width of the liquid–vapor interface is about 4σ; at $T^r = 1.117$ it is about 6σ. Thus, the onset of the asymptotic density behavior obtains for a film whose half-width is a little greater than the width of the corresponding liquid–vapor interface at the same temperature. For smaller half-widths the difference $n_R^r - n_0^r$ increases with increasing $1/\Delta x_{1/2}^r$ faster than the third power. This is because a smaller film results from increasing μ and a consequent increase in $n_R^2 K_T^R(n_R - n_B)$.

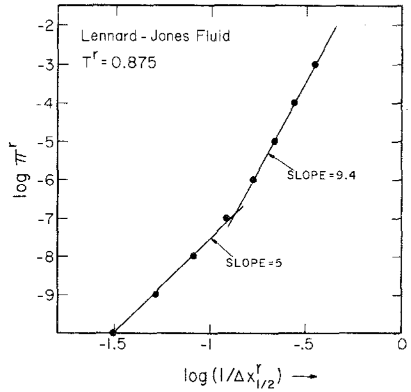

Fig. 9. Gradient-theoretical disjoining pressure versus film half-width.

The logarithm of the reduced disjoining pressure ($\Pi^r = \pi\sigma^3/\epsilon$) predicted by gradient theory is plotted versus the logarithm of $1/\Delta x^r_{1/2}$ in Figs. 9 and 10. The curve is linear in the region in which $n^r_R - n^r_0$ had the expected inverse-cube dependence on film width. However, the slope is about 5 instead of the expected value of 3. This discrepancy between gradient theory and the RK theory could arise from the fact that the boundary phases are only asymptotically uniform, with boundary zones that change in density profile with changing film thickness. Since pressure is a much more sensitive function of chemical potential than density, the disjoining pressure can reflect the changes of the boundary region more strongly than does the density. If this is the origin of the discrepancy, then our results imply that the RK asymptotic theory will be valid only if the boundary phases are solids or fluids totally immiscible with the film material. We cannot of course rule out the possibility that the discrepancy

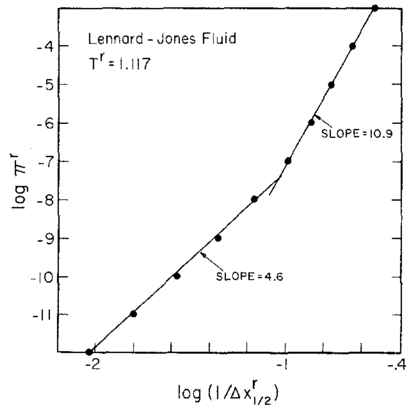

Fig. 10. Gradient-theoretical disjoining pressure versus film half-width.

arises from the approximate nature of the Weeks–Chandler–Andersen theory used for the free energy and pair correlation function. However, whereas their theory should be more accurate at $T^r = 0.875$ than at $T^r = 1.117$ (because the thick films and reference fluid are at higher densities), the discrepancy in slope is larger at $T^r = 1.117$. In the future, we plan to use molecular dynamical data to perform the same calculations to try to resolve the issue.

4. LAYERED STRUCTURES

One-dimensional periodic structures, i.e., layered structures, are also predicted by gradient theory. For a one-component fluid the boundary conditions determining a layered structure are

$$\left.\frac{dn}{dx}\right|_{x_a} = \left.\frac{dn}{dx}\right|_{x_a+\lambda} = 0 \qquad \text{or} \qquad \omega(n_a) = \omega(n_b) \tag{4.1}$$

where $n(x_a) = n_a$, the density minimum; $n(x_a + \lambda) = n_b$, the density maximum; and λ is the half-wavelength of the structure. Certain kinds of liquid crystals are examples of one-dimensional periodic fluid microstructures occurring in nature.

For a given temperature T and chemical potential μ, a periodic structure will be defined for any density pair n_a, n_b for which $\omega(n_a) - \omega(n_b)$ and $\Delta\omega(n) = \omega(n) - \omega(n_a) > 0$ for $n_a < n < n_b$, the latter condition on $\omega(n)$ being forced by Eq. (2.13). Geometrically, $\Delta\omega(n)$ is the vertical height between the curve $f_0(n)$ and the straight line which cuts the curve $f_0(n)$ at n_a and which is parallel to the chemical potential μ. The straight line, which has the equation $n\mu + \omega(n_a)$, is shown in Fig. 11 for three different layered

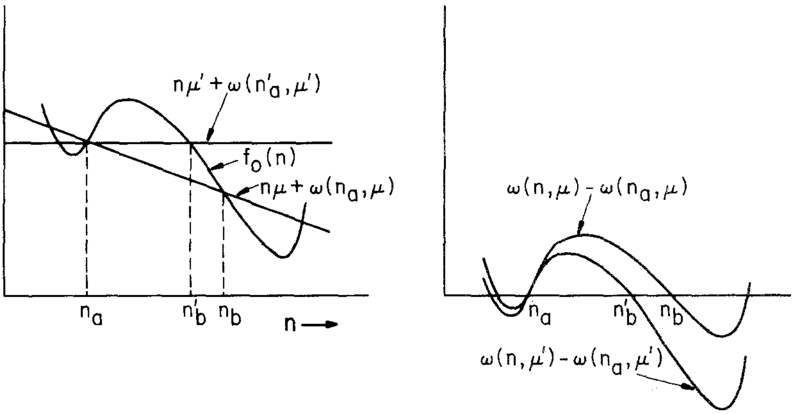

Fig. 11. Free energy construction of the characteristic densities of layered structures.

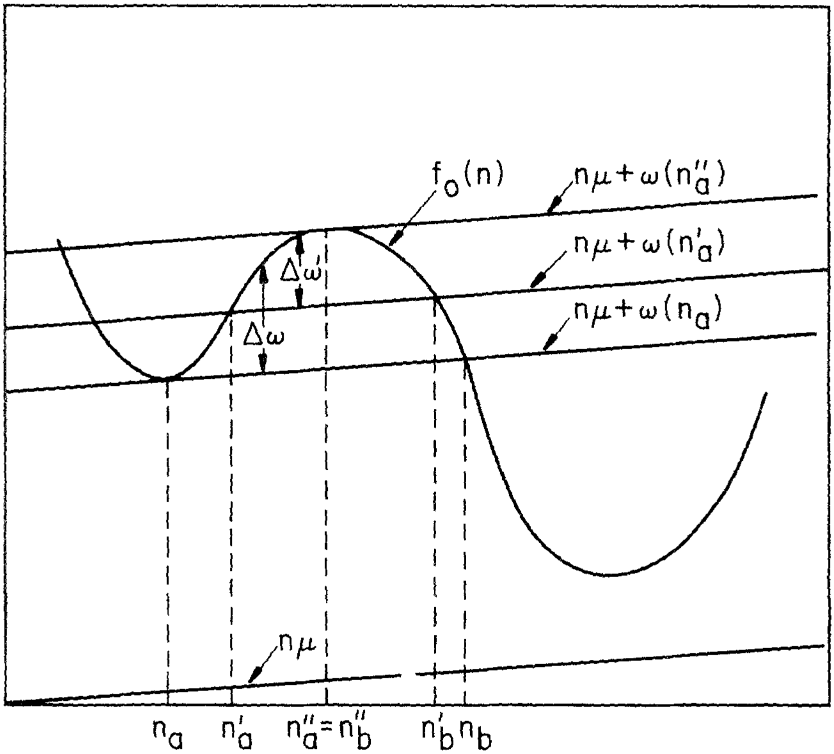

Fig. 12. Free energy construction of the characteristic densities of layered structures.

structures. These structures have the same temperature and chemical potential, but different wavelengths λ and density pairs n_a, n_b. From Fig. 11, it follows that for a given T and μ, layered structures are obtained for any straight line parallel to $n\mu$, provided the minimum density lies between the value n_a at which the line is tangent to $f_0(n)$ and the value n''_a above which the line lies above the dome of $f_0(n)$. The layered structure corresponding to the density pair n_a, n'_b in Fig. 11 is also a thin film. A thin film then is a degenerate case (one of infinite wavelength) of a layered structure, as also is the liquid–vapor interface in the special case that the chemical potential equals that of coexisting liquid and vapor phases. In Fig. 12, we illustrate $\Delta\omega(n)$ for two layered structures at the same temperature and having the same minimum density n_a but different chemical potentials. Their maximum densities have to be different also.

The quantities characterizing a layered structure are T, μ, n_a, n_b, and λ. Here, T must lie below the critical point to satisfy Eq. (4.1) with $\Delta\omega(n) > 0$ for $n_a < n < n_b$. To uniquely determine a layered structure, three of the five

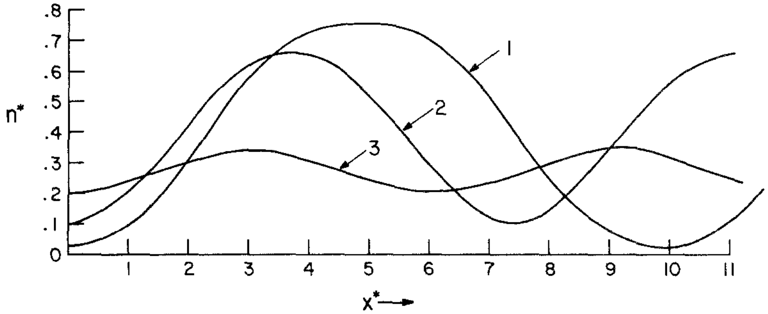

Fig. 13. Density profiles of layered structures of a van der Waals fluid at $T^* = 0.170$. Curve 1 corresponds to the conditions $n_a^* = 0.030$ and $\mu^* = -0.732$, curve 2 to $n_a^* = 0.100$ and $\mu^* = -0.732$, and curve 3 to $n_a^* = 0.200$ and $\mu^* = -0.650$.

quantities T, μ, n_a, n_b, and λ must be set. Thus, for a layered structure in a one-component fluid, there are three degrees of freedom.

In reduced coordinates the profile equation for a layered structure in a van der Waals fluid is

$$x^* - x_a^* = \frac{1}{\sqrt{2}} \int_{n_a^*}^{n^*(x^*)} \frac{dn^*}{\left[\omega^*(n^*) - \omega^*(n_a^*)\right]^{1/2}} \tag{4.2}$$

The half-wavelength λ^* and tension are given by

$$\lambda^* = \frac{1}{\sqrt{2}} \int_{n_a^*}^{n_b^*} \frac{dn^*}{\left[\omega^*(n^*) - \omega^*(n_a^*)\right]^{1/2}} \tag{4.3}$$

and

$$\gamma^* = 2\sqrt{2} \int_{n_a^*}^{n_b^*} \left[\omega^*(n^*) - \omega^*(n_a^*)\right]^{1/2} dn^* \tag{4.4}$$

The tension and wavelengths are given in Table III for a few layered structures of a van der Waals fluid at $T^* = 0.170$. Three corresponding density profiles are shown in Fig. 13. The trends illustrated by Table III are that tension increases with decreasing chemical potential if n_a is fixed and that tension decreases with increasing n_a (or decreasing n_b) at constant chemical potential.

Properties of a sequence of layered structures corresponding to the same chemical potential are given in Fig. 14 and Table IV for the 6–12 Lennard-Jones fluid. The structures are quite similar to those of the van der Waals fluid. As expected, $\lambda^r = \infty$ in the thin-film limit and $\gamma^r = 0$ in the limit $n_a^r = n_b^r$.

Table III. Reduced Minimum and Maximum Densities n_a^* and n_b^*, Wavelength l*, Tension g* and Chemical Potential m* of a van der Waals Fluid at $T^* = 0.170$

n_a^*	n_b^*	μ^*	λ^*	γ^*
0.0300	0.7599	− 0.7317	4.75	0.298
0.1000	0.6650	− 0.7317	3.75	0.207
0.3000	0.4437	− 0.7317	2.75	0.015
0.0300	0.4658	− 0.6500	4.95	0.113
0.1000	0.4319	− 0.6500	3.10	0.074
0.200	0.3466	− 0.6500	3.10	0.015

There is an interesting feature of the wavelength λ of a layered structure. For a given value of μ, as n_a and n_b approach each other at the point n_B where $\mu = (\partial f_0/\partial_n)(n_B)$ [and $(\partial^2 f_0/\partial n^2)(n_B) < 0$], the tension of the structure tends to zero, whereas λ approaches a finite value λ_B. To see this property analytically, consider the expression

$$x - x_a = \frac{1}{\sqrt{2}} \int_{n_a}^{n(x)} \frac{\sqrt{c}\, dn}{\left[\omega(n) - \omega(n_a)\right]^{1/2}} \tag{4.5}$$

For n_a and n_b sufficiently close to n_B, the terms $c(n)$, $\omega(n)$, and $\omega(n_a)$ can be expanded about n_B. With the condition $[\partial\omega(n)/\partial n]|_{n_B} = 0$, to lowest order

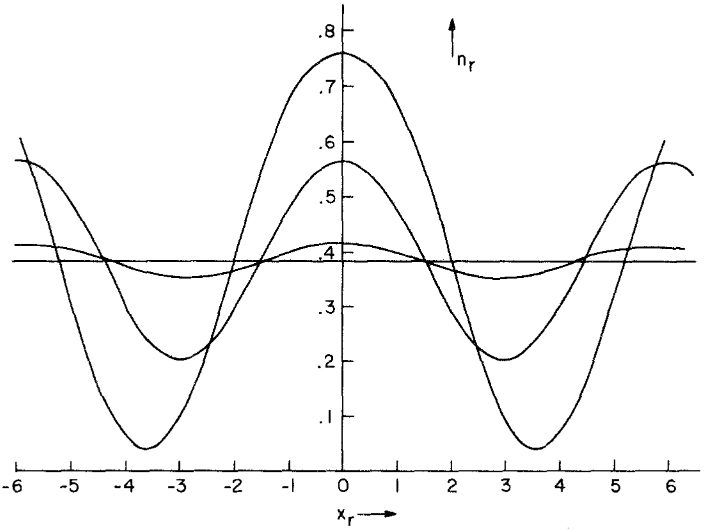

Fig. 14. Density profiles of layered structures of a 6–12 Lennard-Jones fluid at $T^r = 0.703$ and $\mu^r = -4.366$.

Table IV. Reduced Minimum and Maximum Densities n_a^r and n_b^r, Wavelength l^r (≡ l/s), and Tension g^r of Layered Structures of a 6–12 Lennard-Jones Fluid at Fixed Temperature (T^r = 0.703) and Chemical Potential (m^r = −4.366)

n_a^r	n_b^r	λ^r	γ^r
0.00205	0.842	∞	3.0269
0.00222	0.8416	13.75	3.026
0.00302	0.839	11.53	3.025
0.00404	0.835	10.63	3.021
0.00807	0.823	9.29	2.992
0.0202	0.796	8.06	2.864
0.0404	0.761	7.31	2.608
0.0807	0.704	6.65	2.079
0.202	0.565	5.98	0.768
0.303	0.460	5.82	0.0148
0.365	0.397	5.792	0.0063
0.375	0.3874	5.7906	0.0009
0.378	0.3844	5.7909	0.0002
0.381	0.381	5.7905	0

in $(n_a - n_b)$ and $(n - n_B)$, Eq. (4.5) becomes

$$x - x_a = \left[-\frac{1}{c(n_B)} \frac{\partial^2 f_0}{\partial n^2}(n_B) \right]^{-1/2} \int_{n_a}^{n(x)} \frac{dn}{\left[(n_B - n_a)^2 - (n - n_B)^2 \right]^{1/2}} \tag{4.6}$$

The solution to this equation is

$$x - x_a = \left[-\frac{1}{c(n_B)} \frac{\partial^2 f_0}{\partial n^2}(n_B) \right]^{1/2} \left[\sin^{-1}\left(\frac{n(x) - n_B}{n_B - n_a} \right) + \frac{\pi}{2} \right] \tag{4.7}$$

or, inverted,

$$\frac{n(x) - n_B}{n_B - n_a} = \sin\left\{ \left[-\frac{1}{c(n_B)} \frac{\partial^2 f_0}{\partial n^2}(n_B) \right]^{1/2} (x - x_a) - \frac{\pi}{2} \right\} \tag{4.8}$$

The value of λ is determined by setting $n(x) = n_b$ on the rhs of Eq. (4.7). In the limit that $n_a \to n_{B^-}$ and $n_b \to n_{B^+}$, Eq. (4.7) yields for λ_B the value

$$\lambda_B = \left[-\frac{1}{c(n_B)} \frac{\partial^2 f_0}{\partial n^2}(n_B) \right]^{-1/2} \tag{4.9}$$

The tension of the film corresponding to Eq. (4.7) is

$$\gamma = \frac{1}{2\lambda_B}(n_B - n_a)^2\left\{\sin^{-1}\left(\frac{n_b - n_B}{n_B - n_a}\right) + \frac{\pi}{2} + \frac{1}{2}\frac{n_b - n_B}{n_B - n_a}\left[1 - \left(\frac{n_b - n_B}{n_B - n_a}\right)^2\right]^{1/2}\right\} \tag{4.10}$$

a result showing that $\gamma \to 0$ faster than $(n_B - n_a)^2$ as n_a and n_b approach n_B.

Even though layered structures of a one-component fluid are not thermodynamically stable, the small-amplitude, low-excess-free-energy (i.e., low-tension) structures described by Eqs. (4.8) can be present as thermal fluctuations or as transients in a freezing fluid. In fact, in the theory of the spinodal decomposition of a rapidly cooled homogeneous phase, Cahn(21) found that microstructures of separating phases of characteristic length λ_B form preferentially in the initial stages of cooling. From the theory given here, we see that this occurs because the low-excess-free-energy structures have characteristic lengths clustered around λ_B.

5. CONCLUDING REMARKS

We have outlined the general fluid gradient theory of microstructures for multicomponent systems. Equilibrium structures are determined by the extremal equations of F, Eq. (2.11) or (2.19) for the present theory. These structures represent stable equilibrium if the second variation of F is positive for mass-conserving fluctuations, i.e., if

$$\sum_{\alpha,\beta}\int\int \frac{\delta^2 F(\{\mathbf{n}\})}{\delta n_\alpha(\mathbf{r})\,\delta n_\beta(\mathbf{r}')} v_\alpha(\mathbf{r}) v_\beta(\mathbf{r}')\, d^3r\, d^3r' > 0 \tag{5.1}$$

for arbitrary density fluctuations $v_1, \ldots, v_\nu$, not all zero and such that $\int v\, d^3r = 0$; $\alpha = 1, \ldots, \nu$. The symbol $\delta(\;)/\delta n(r)$ denotes a functional derivative with respect to $n(\mathbf{r})$. Although we do not present the analysis here, we have shown that planar thin films and layered structures of one-component fluids are not thermodynamically stable. Nevertheless, since the gradient theory of stable microstructures of multicomponent fluids will be similar in qualitative and mathematical detail to that of one-component fluid microstructures, we feel the results given in the preceding sections provide a useful step in the development of the general theory of fluid microstructures. In a separate work(22) we have addressed the question of the origins and nature of stability of fluid microstructures.

ACKNOWLEDGMENT

We acknowledge V. Bongiorno, who was involved in the early stage of the research reported herein. We are grateful to NSF and DOE for financial support of this research.

REFERENCES

1. Lord Rayleigh, *Phil. Mag.* **33**:209 (1892).
2. J. D. van der Waals and Ph. Kohnstamm, *Lehrbuch der Thermodynamik* (Mass and van Suchtelen, Leipzig, 1908), Vol. I.
3. J. W. Cahn and J. E. Hilliard, *J. Chem. Phys.* **28**:258 (1958).
4. V. Bongiorno and H. T. Davis, *Phys. Rev. A* **13**:2213 (1973).
5. V. Bongiorno, L. E. Scriven, and H. T. Davis, *J. Colloid Interface Sci.* **57**:462 (1976); A. H. Falls, L. E. Scriven, and H. T. Davis, *J. Chem. Phys.* (submitted for publication).
6. B. M. McCoy and H. T. Davis, *Phys. Rev. A* **20**: 1201 (1979).
7. B. S. Carey, L. E. Scriven, and H. T. Davis, *AIChE J.* **24**:1076 (1978); (1979) (to be published).
8. A. J. M. Yang, P. D. Fleming III, and J. H. Gibbs, *J. Chem. Phys.* **64**:3732 (1976); P. D. Fleming III, A. J. M. Yang, and J. H. Gibbs, *J. Chem. Phys.* **65**:7 (1976).
9. B. S. Carey, L. E. Scriven, and H. T. Davis, *J. Chem. Phys.* **69**:5040 (1978).
10. B. F. McCoy, L. E. Scriven, and H. T. Davis, *J. Chem. Phys.* (to be published).
11. R. Bearman and J. G. Kirkwood, *J. Chem. Phys.* **28**:136 (1958).
12. H. T. Davis and L. E. Scriven, *J. Chem. Phys.* **69**:5215 (1978).
13. F. H. Stillinger, Jr. and A. Ben-Naim, *J. Chem. Phys.* **47**:4431 (1967).
14. J. D. Weeks, D. Chandler, and H. C. Andersen, *J. Chem. Phys.* **54**:5237 (1971); *Phys. Rev. A* **4**:1597 (1971).
15. B. Widom, *J. Chem. Phys.* **62**:1332 (1975).
16. J. C. Melrose, *SCI Monograph* No. 25 (1967), p. 123.
17. B. V. Deryagin, *Zh. Fiz. Khim.* **5**:379 (1934).
18. B. V. Deryagin and Kussakov, *Bull. Acad. Sci. USSR* **1936**:471; *Acta Physicochim.* **10**:25 (1939).
19. A. Sheludko, *Adv. Coll. Interface Sci.* **1**:391 (1967).
20. A. I. Rusanov and F. M. Kuni, in *Research in Surface Forces*, V. B. Deryagin, ed. (Consultants Bureau, N.Y., 1971), Vol. 3, p. 111.
21. J. W. Cahn, *J. Chem. Phys.* **42**:93 (1965).
22. H. T. Davis and L. E. Scriven, *Adv. Chem. Phys.* (1981) (to appear).